

Article

# Preparation, Characterization and Antioxidant Activities of Kelp Phlorotannin Nanoparticles

Ying Bai <sup>1</sup>, Yihan Sun <sup>1</sup>, Yue Gu <sup>1</sup>, Jie Zheng <sup>2</sup>, Chenxu Yu <sup>3</sup> and Hang Qi <sup>1,\*</sup> 

<sup>1</sup> School of Food Science and Technology, Dalian Polytechnic University, National Engineering Research Center of Seafood, Liaoning Provincial Aquatic Products Deep Processing Technology Research Center, Dalian 116034, China; 18340837366@163.com (Y.B.); s18641423774@163.com (Y.S.); 713guyue@sina.com (Y.G.)

<sup>2</sup> Liaoning Ocean and Fisheries Science Research Institute, Dalian 116023, China; zhengjiesd@163.com

<sup>3</sup> Department of Agricultural and Biosystems Engineering, Iowa State University, Ames, IA 50011, USA; chenxuyu@iastate.edu

\* Correspondence: qihang@dlpu.edu.cn; Tel.: +86-411-86318785

Academic Editor: Petras Rimantas Venskutonis

Received: 27 August 2020; Accepted: 1 October 2020; Published: 5 October 2020



**Abstract:** Phlorotannins are a group of major polyphenol secondary metabolites found only in brown algae and are known for their bioactivities and multiple health benefits. However, they can be oxidized due to external factors and their bioavailability is low due to their low water solubility. In this study, the potential of utilizing nanoencapsulation with polyvinylpyrrolidone (PVP) to improve various activities of phlorotannins was explored. Phlorotannins encapsulated by PVP nanoparticles (PPNPS) with different loading ratios were prepared for characterization. Then, the PPNPS were evaluated for in vitro controlled release of phlorotannin, toxicity and antioxidant activities at the ratio of phlorotannin to PVP 1:8. The results indicated that the PPNPS showed a slow and sustained kinetic release of phlorotannin in simulated gastrointestinal fluids, they were non-toxic to HaCaT keratinocytes and they could reduce the generation of endogenous reactive oxygen species (ROS). Therefore, PPNPS have the potential to be a useful platform for the utilization of phlorotannin in both pharmaceutical and cosmetics industries.

**Keywords:** phlorotannin; encapsulation; characterization; stability; antioxidant activity

## 1. Introduction

In recent years, research on bioactive substances originated from algae has increased rapidly. These compounds not only can serve as preservatives and antioxidant protectants in food and cosmetics, but also show multiple health benefits [1]. Among these active compounds, polyphenolic phlorotannins, a group of complex molecular assemblages from the polymerization of phloroglucinol [2], represent a large class of well-characterized brown algae secondary metabolites [3]. They have been revealed to have a range of diverse biological functions and activities, such as antibacterial [4], anti-inflammatory [5], anti-oxidant [6], antidiabetic [7], anti-HIV [8] and anticancer [9–11] activities. However, phlorotannins are highly sensitive to external factors such as light, pH, heat and oxidative reagents, which limit their applications in food, cosmetic, nutraceutical and pharmaceutical industries [12]. In addition, low water solubility of phlorotannin leads to low absorption in the gastrointestinal tract, which affects their bioavailability [13,14].

Encapsulation is a common technique to wrap a core material with functional activity in a coating material to form a capsule. This technology can not only mask or retain flavor and increase solubility, but also protects the core material from degradation by environmental factors and controls the release of various biologically active compounds at the target site [15]. Solid dispersion technique is one of the encapsulation methods that has been applied to various drugs and natural bioactive substances [16].

To apply such a technique on phlorotannin, it is important to fully investigate the effects of encapsulation on the functional properties of phlorotannin. In the preparation of solid dispersion, a water-soluble carrier such as high-molecular-weight polyvinylpyrrolidone (PVP) would be a good choice as it has low toxicity, good physiological compatibility and excellent thermophysical properties which will facilitate its application in medicine, food and cosmetics [17]. PVP is an amorphous, polar polymer, well soluble in water and some organic solvents, and is able to form complexes with other substances. It is also a good stabilizer, which can prevent the aggregation of nanoparticles through the repulsive force formed by its hydrophobic carbon chains, which extend into the solvents and interact with each other [18]. These characteristics make PVP possess better wall material advantages in preparing nanoparticles compared other chemicals. The objectives of this study were two-fold: (1) to characterize physicochemical properties of phlorotannin encapsulated with PVP nanoparticles (PPNPS) and to evaluate the improvement over stability and the retention rate of active phlorotannins by PPNPS in the *in vitro* digestion process; and (2) to analyze the PPNPS cytotoxicity and antioxidant activities using a keratinocyte model to evaluate the potential of PPNPS as an anti-oxidative protectant, which potentially can be used in skincare products.

## 2. Results and Discussion

### 2.1. Characterization of PPNPS

In order to evaluate the stability of the PPNPS, the nanoparticles were prepared with different loading ratios of phlorotannin:PVP. As shown in Figure 1a, images of PPNPS samples with different loading indicated that as the PVP concentration increased, the color of the PPNPS became lighter. This suggested that more and more phlorotannins were embedded inside the PVP shell and fewer exposed phlorotannins remained on the surface of the PPNPS. These results were consistent with the embedding rate from 1:6 to 1:16 (phlorotannin: PVP, *w/w*) analyzed using high-performance liquid chromatography (HPLC, Shimadzu SPD 20A, Kyoto, Japan). The embedding rates were  $89.56 \pm 1.21\%$ ,  $89.22 \pm 0.81\%$ ,  $88.56 \pm 1.35\%$ ,  $88.92 \pm 1.15\%$  and  $89.47 \pm 1.32\%$ , respectively (1:6, 1:8, 1:10, 1:12, 1:16) (data not shown).

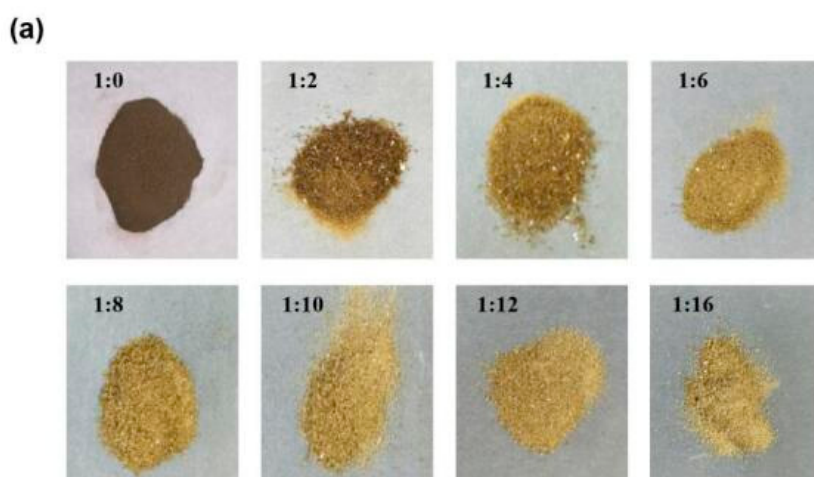
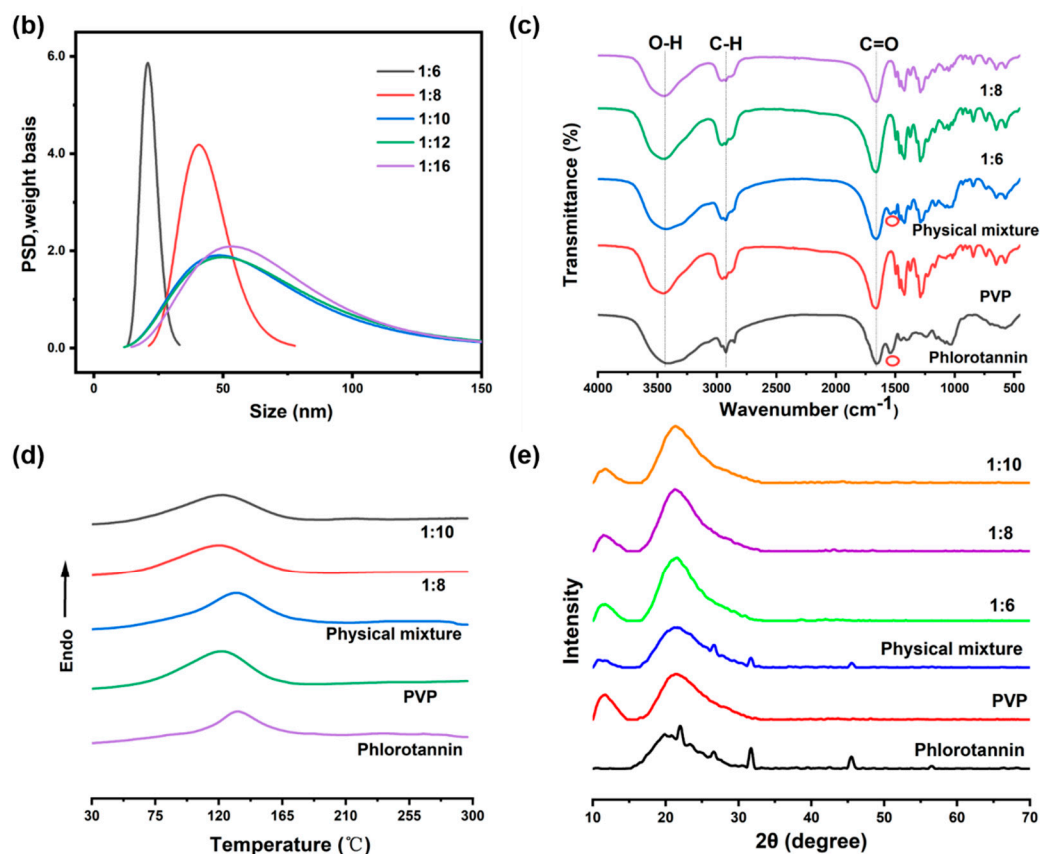


Figure 1. Cont.



**Figure 1.** Characterization of PPNPS (polyvinylpyrrolidone nanoparticles): (a) Images of PPNPS with different loading ratios; (b) Particle size distribution (the concentration of PPNPS was 10 mg/mL in solution); (c) FTIR spectra (the samples were solid); (d) DSC (differential scanning calorimetry) thermograms (the samples were solid) and (e) X-ray diffraction patterns (the samples were solid).

Particle size distribution (Figure 1b) of PPNPS with loading ratios of phlorotannin:PVP ( $w/w$ ) of 1:6, 1:8, 1:10, 1:12, 1:16 ( $w/w$ ) showed that as the PVP content increased, the average size of the PPNPS appeared to gradually increase, while the uniformity of the PPNPS declined and broader distribution was observed. It is reasonable that as the PVP concentration gradually increased, the shell became thicker.  $D_{50}$  values of 1:6, 1:8, 1:10, 1:12, 1:16 were  $20.84 \pm 0.94$ ,  $40.62 \pm 2.55$ ,  $48.32 \pm 2.39$ ,  $49.66 \pm 2.71$ ,  $53.17 \pm 2.47$  nm, respectively. This suggested that encapsulation of PVP caused an expansion of the nanoparticles, which is a common phenomenon reported in the literature [19]. The FTIR measurement was performed to verify the encapsulation of phlorotannin inside the PVP shell [20]. As shown in Figure 1c, when the FTIR spectra of the PPNPS, phlorotannin and phlorotannin + PVP mixture were compared, it was clear that some of the peaks associated with specific functional groups in the phlorotannin molecules (e.g.,  $1546\text{ cm}^{-1}$ ) only appeared in the spectrum of the mixture, but not in that of the PPNPS. Apparently, the encapsulation of the phlorotannin was successful in the PPNPS (1:6 and 1:8) and only the PVP (the shell in the PPNPS) bands were observed in the representative FTIR spectrum of PPNPS. However, the FTIR spectrum of the physical mixture sample showed both phlorotannin and PVP characteristic peaks. These characteristic peaks in the physical mixture samples also supported the encapsulation of phlorotannin. The result was similar to Zhu et al.'s previous report that fucoxanthin had been successfully encapsulated in heteroprotein complex coacervates [21]. The FTIR spectra revealed that phlorotannin had a broad absorption peak around  $3410\text{ cm}^{-1}$  due to the O-H stretching vibrations [22]. An absorption band of the carbonyl group from PVP was detected around  $1658\text{ cm}^{-1}$  [23]. Phlorotannin was bound to PVP by hydrogen bonds between the hydroxyl group of phlorotannin and the carbonyl group of PVP. The bond was responsible for the cross-linking

of the two compounds, facilitating their precipitation in the alcohol solution and the formation of PPNPS [23].

The DSC (differential scanning calorimetry) thermogram of phlorotannin presented an endothermic peak at 130 °C, indicating its melting point, as shown in Figure 1d. PVP is an amorphous polymer and, for this reason, it did not present a clear melting peak. Therefore, the endothermic peak present was attributed to the evaporation of residual moisture. An endothermic peak of phlorotannin could not be seen in the nanoparticles, probably due to the low phlorotannin concentration and its encapsulation by PVP. X-ray diffractometry is a useful way to determine the crystalline formation for the nutrients or drugs encapsulated between nanoparticles [24]. The XRD (X-ray diffractometry) analysis of PPNPS was performed as shown in Figure 1e. Phlorotannin showed major sharp peaks at  $2\theta$  diffraction angles 20° and 50°, which confirmed the phlorotannin's crystalline nature. The XRD pattern of pure PVP did not show crystalline peaks because PVP is an amorphous polymer. Meanwhile, in the physical mixture spectrum, the characteristic phlorotannin peaks with a low level were also found at the same positions as that in phlorotannin powder, indicating that phlorotannin in the mixture is also crystalline. However, crystalline peaks disappeared in the XRD pattern of PPNPS at the ratio of 1:6, 1:8 and 1:10. In fact, this crystallinity modification could be attributed to PVP, which may have surrounded the crystal aggregates of phlorotannin during the preparation of PPNPS, thus forming an amorphous shell [25]. These results are consistent with previous reports which showed that the physical state of lutein was converted from crystalline to amorphous due to encapsulation and the chemical interactions between lutein and PVP during nanoparticle preparation [20]. These characterization results combined with the embedding rate of phlorotannin show that the ratio of 1:8 would be appropriate for making PPNPS based on its good particle size and effective embedding rate.

Figure 2 presents the transmission electron microscopy (TEM) image of PPNPS in a phlorotannin:PVP mass ratio of 1:8 (*w/w*). The TEM image shows highly uniform and monodisperse nanoparticles without agglomeration [26] and which were mainly composed of spherical nanoparticles, similar to the results reported by do Prado Silva, J.T. et al. [23]. Most particles were visible at ~40–50 nm, which was consistent with the particle size results.

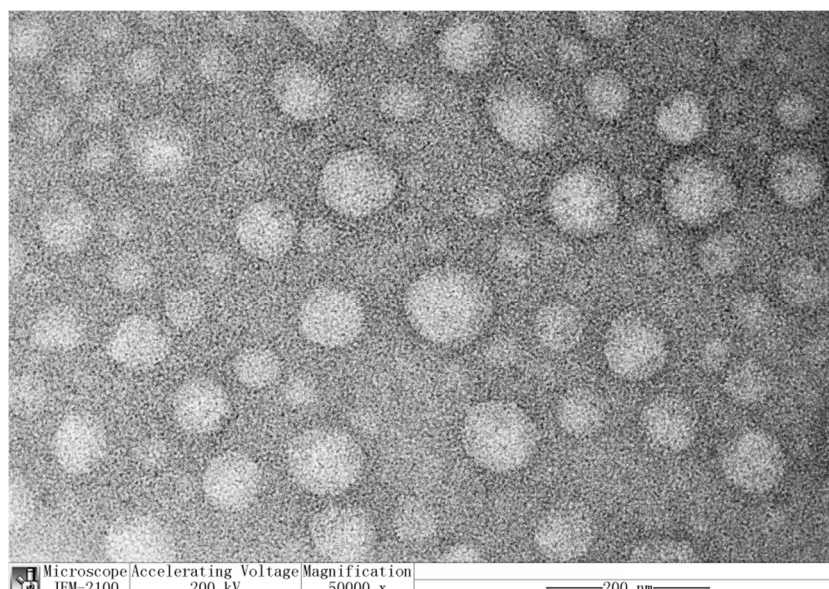


**Figure 2.** TEM (transmission electron microscopy) images of PPNPS. The concentration of PPNPS was 1 mg/mL.

## 2.2. Stability of Phlorotannin

The storage stability of phlorotannin was evaluated under the same conditions over a 15-day duration, as shown in Figure 3. The original state of phlorotannin and PPNPS (1:6, 1:8, 1:10) were incubated in glass tubes with the same amounts. After adding the same amount of water and mixing samples, the PPNPS were dissolved in water. However, phlorotannin did not dissolve in the water and formed a green suspension that was prone to sedimentation as shown in Figure 3. After incubation for 5 days at room temperature ( $22 \pm 3 \text{ }^\circ\text{C}$ ), the PPNPS were stable in water without precipitation. This phenomenon was also found after standing for 10 days and 15 days. These results suggest that the deposition rate of phlorotannin out of the nanoparticles was very low. The PVP-embedded phlorotannin, on the other hand, could be uniformly dissolved in water. For dispersions, no precipitation was observed, indicating the absence of phlorotannin expulsion from PVP. These results indicate that encapsulation effectively improved the stability of phlorotannin. This proved that the deposition rate of nanoencapsulated phlorotannin was lower than that of unembedded ones. It also showed that the stability of the product was quite good. Similar detection methods and results were also reported in the study of astaxanthin-loaded core-shell nanoparticles consisting of chitosan oligosaccharides and poly (lactic-co-glycolic acid) [27].

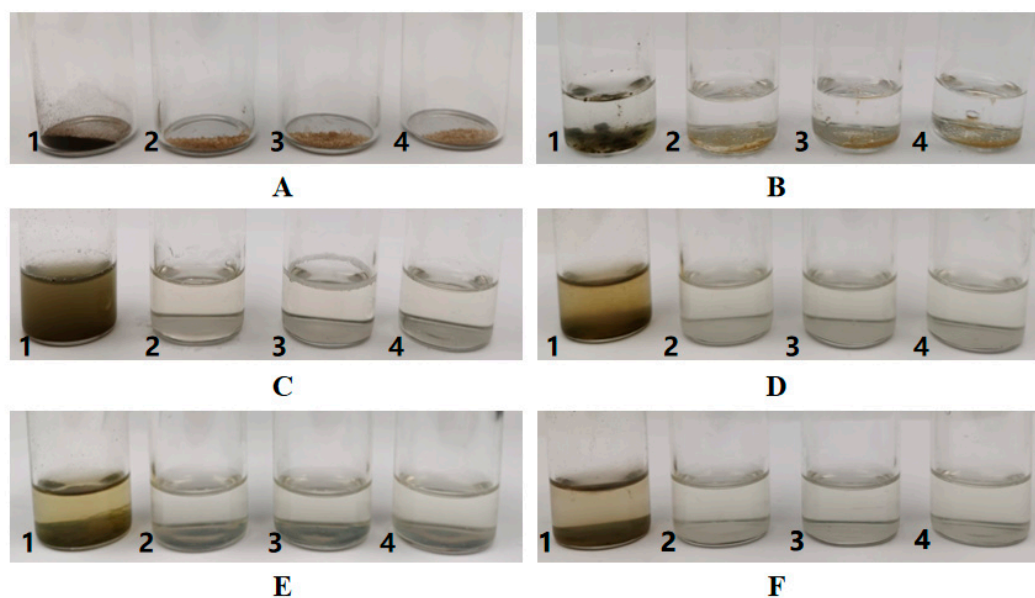


**Figure 3.** Stability of free phlorotannin (1) and PPNPS (1:6(2), 1:8(3), 1:10(4)) at room temperature ( $22 \pm 3 \text{ }^\circ\text{C}$ ) (A: Original state; B: Adding water; C: Mixture; D: Standing for 5 days; E: Standing for 10 days; F: Standing for 15 days). The concentration of every sample was 20 mg/mL (100 mg solid sample mixed with 5 mL water).

## 2.3. Controlled Release of Phlorotannin

An *in vitro* release profile is usually used to predict *in vivo* behavior, drug dosage, release mechanism and kinetics of encapsulated drugs [25]. As shown in Figure 4, the release characteristics of free phlorotannin and phlorotannin from the PPNPS under simulated gastrointestinal conditions were studied. Free phlorotannin showed a  $39.68 \pm 2.96\%$  burst release within 2 h in a simulated gastric fluid (SGF). Subsequently, it was continuously released in a simulated intestinal fluid (SIF) in the next 4 h and the final cumulative percentage of the released phlorotannin reached  $94.72 \pm 1.37\%$ . In contrast, under simulated gastrointestinal conditions, phlorotannin in PPNPS showed slower and sustained release kinetics with a total release percentage of approximately  $52.76 \pm 0.94\%$ . Based on these results, PVP as a shell material could slow down the release rate of phlorotannin. As shown in other investigations, encapsulation with PVP is an approach for enhancing the stability

and bioavailability of poorly water soluble drugs [28] and our results were consistent with this research. Other investigations reported the slow release in gastrointestinal conditions of other bioactive compounds such as curcumin [29], thyme essential oil [30], phloretin [19] and fucoxanthin [31], which were also in agreement with our study.

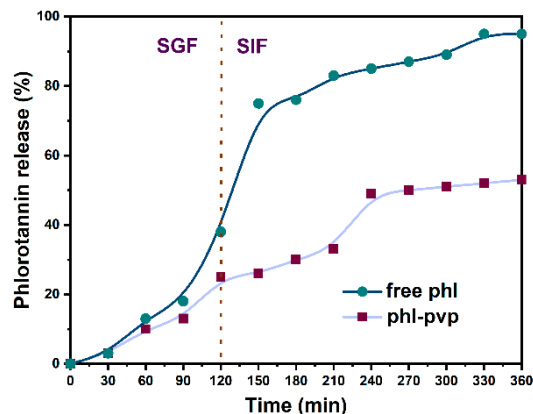


**Figure 4.** Release profile of free phlorotannin and PPNPS (1:8, *w/w*) in simulated gastrointestinal fluids.

#### 2.4. Antioxidant Activity and Cytotoxicity of PPNPS

Overexposure to reactive oxygen species (ROS) can cause oxidative stress, which can damage essential cell macromolecules (such as proteins, lipids and DNA), thereby increasing risks of several chronic human diseases such as cancer, inflammation and neurodegenerative diseases [32]. Hydrogen peroxide ( $H_2O_2$ ) can induce oxidative damage to cells by increasing the production of ROS. We hypothesized that PPNPS may have protective effects on  $H_2O_2$ -induced oxidative damage. To test this hypothesis, the production of ROS was measured in HaCaT keratinocytes (Figure 5) upon peroxide treatments. Fluorescent images of HaCaT keratinocytes stained with  $H_2DCFDA$  probes were shown in Figure 5a–d. In the fluorescence images, the  $H_2O_2$  treatment group had the strongest fluorescence intensity and after the PPNPS treatment the fluorescence decreased. As expected,  $H_2O_2$  treatment significantly increased cellular ROS production in HaCaT keratinocytes, while PPNPS treatment significantly reduced ROS production. When the concentrations of PPNPS treatment were 6.25 and 12.5  $\mu\text{g/mL}$ , the proportion of ROS production decreased by 12 and 18%, respectively. The results are consistent with previous reports that phlorotannin could be developed as a potential ROS inhibitor [33]. In terms of the effect on cell viability, the cell viability of HaCaT keratinocytes treated with 1 mM hydrogen peroxide was  $47.90 \pm 1.49\%$ , and that of HaCaT keratinocytes treated with 6.25 and 12.5  $\mu\text{g/mL}$  PPNPS significantly increased to  $60.02 \pm 2.50\%$  and  $75.71 \pm 1.51\%$  ( $p < 0.05$ ), respectively. That meant that PPNPS could improve the cell viability of oxidized HaCaT keratinocytes and could be potentially used in skin antioxidants. The cytotoxicity of the PPNPS was determined using HaCaT keratinocytes. Four selected concentrations of 6.25, 12.5, 25 and 50  $\mu\text{g/mL}$  PPNPS (1:8, *w/w*) were incubated with HaCaT keratinocytes for 24 h to detect whether PPNPS could produce any toxic effects. As shown in Figure 5f, the cell viabilities of the four concentrations were  $100.54 \pm 4.69\%$ ,  $101.72 \pm 4.01\%$ ,  $104.98 \pm 0.81\%$ ,  $109.88 \pm 2.42\%$ , respectively. The cell viabilities among 6.25, 12.5 and 25  $\mu\text{g/mL}$  PPNPS (1:8, *w/w*) were not significant ( $p > 0.05$ ), but the cell viability significantly increased at the concentration of 50  $\mu\text{g/mL}$  PPNPS (1:8, *w/w*) ( $p < 0.05$ ). These results indicated that PPNPS were not cytotoxic to HaCaT keratinocytes. It can safely be used on skin or as functional chemicals in cosmetics.

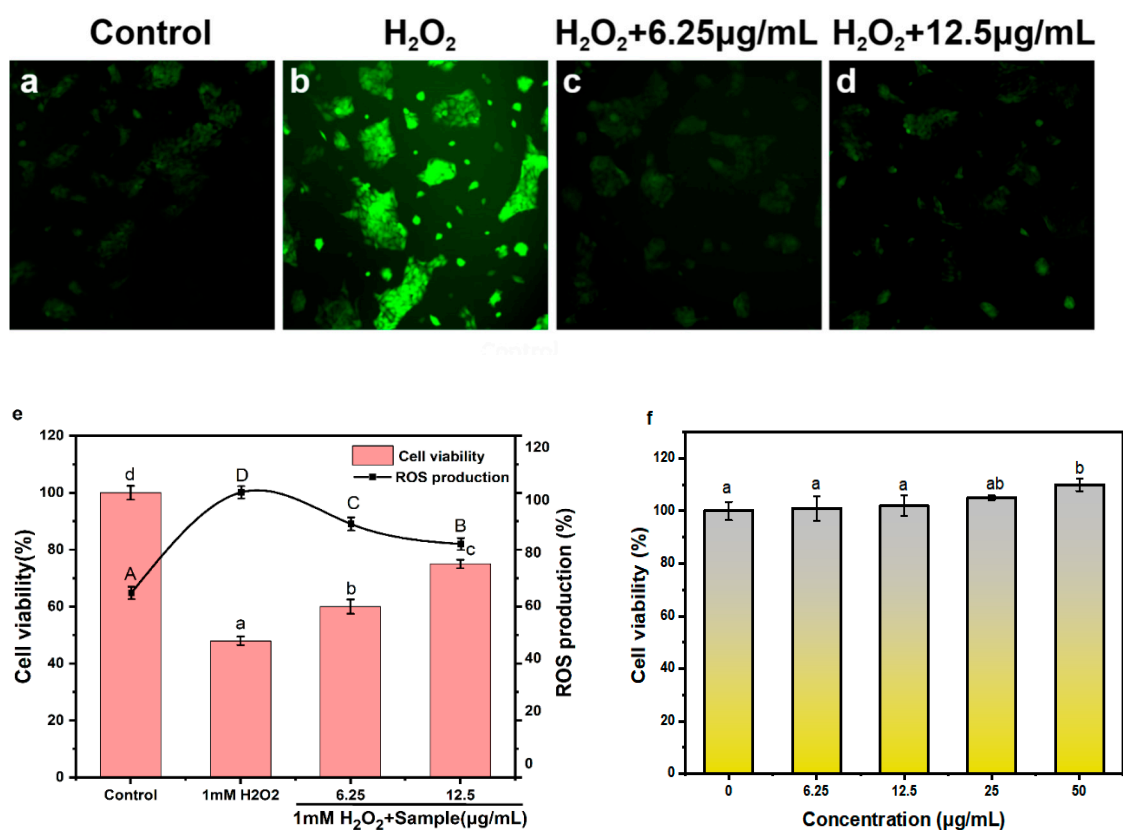


**Figure 5.** Antioxidant activity and cytotoxicity of HaCaT keratinocytes. (a–d) Fluorescent images of HaCaT keratinocytes treated with H<sub>2</sub>O<sub>2</sub> and PPNPS (1:8) and stained with H<sub>2</sub>DCFDA probe. (e) Cell viability and relative fluorescence intensity of HaCaT keratinocytes treated with H<sub>2</sub>O<sub>2</sub> and PPNPS (1:8, *w/w*) at different concentrations. (f) Cytotoxicity of HaCaT keratinocytes treated with PPNPS (1:8, *w/w*) at different concentrations. Data are expressed as the mean ± SD. Multiple group comparisons were performed using one-way ANOVA; data that are not denoted with the same letter are significantly different ( $p < 0.05$ ).

### 3. Materials and Methods

#### 3.1. Samples and Chemicals

Phlorotannin (80% purity) from kelp was obtained from Hubei Yongkuo Technology Co., Ltd. Ethanol (99.5%, Neon) and polyvinylpyrrolidone (40,000 g·mol<sup>-1</sup>, Sigma-Aldrich) were used in the extraction and encapsulation of the phlorotannin. HaCaT keratinocytes came from Shanghai Tongpai Technology Co., Ltd. and were cultured in Dulbecco's Minimum Essential Medium (DMEM), containing 100 U/mL penicillin, 100 U/mL streptomycin and 10% FBS. DMEM and trypsin (0.25% with EDTA) were purchased from Gibco (Thermo Fisher, Fair Lawn, NJ, USA). Penicillin, streptomycin solution and PBS were obtained from HyClone (Logan, UT, USA). Fetal bovine serum (FBS) was obtained from Sangon Biotech Co., Ltd. (Shanghai, China). Dimethyl sulfoxide (DMSO) was obtained from Yeasen Biotech Co., Ltd. (Shanghai, China). MTT and 2',7'-dichlorodihydrofluorescein diacetate (H<sub>2</sub>DCFDA) were obtained from Baoxidia Co., Ltd. (Beijing, China). Pepsin and pancreatin were purchased from Sigma. Other reagents were obtained from Sangon Biotech Co., Ltd. (Shanghai, China).

#### 3.2. Preparation of PPNPS

Initially, PVP was dissolved in ethanol under magnetic stirring until translucent solutions were obtained. Phlorotannin extracts with 80% purity were washed with water until colorless and were centrifuged to discard the supernatant to remove highly polar substances. They were then washed

with  $\text{CHCl}_3$  until colorless to remove weakly polar substances and the obtained purified phlorotannin was dissolved in 100% ethanol. The purified phlorotannins with purity of  $90.24 \pm 4.47\%$  based on Folin–Ciocalteu method were to be used for the next steps. The same weight amounts of phlorotannin in ethanol solution were added in different proportions of PVP translucent solutions which were initially prepared as the ratio of 1:2, 1:4, 1:6, 1:8, 1:10, 1:12, 1:14 (phlorotannin:PVP, *w/w*) were added to phlorotannin solution, and the mixtures were stirred evenly. The obtained mixtures were sonicated for 15 min under pulse condition of 30 s on and 10 s off (Sonics Vibra-Cell™, and 1/8' tip). Finally, the solvent was evaporated in a circulation oven at 30 °C for 24 h, then the samples were freeze-dried in lyophilizer (Scientz-10ND, Zhejiang, China). This nanoparticle-formed mechanism could be due to the hydrogen bond formation between PVP and phlorotannin inside the nanoparticles.

### 3.3. Nanoparticle Characterization

Dispersion Technology (DT Zeta & Size 1202, Dispersion Technology, Inc. Bedford Hills, NY, USA) was used to measure the particle size distribution and mean particle size of the PPNPS. The thermal properties of PPNPS were determined by DSC (DSC250, TA Instrument, New Castle, DE, USA). Nanoparticles, pure compounds (phlorotannin and PVP) and their physical mixture (a phlorotannin:PVP ratio of 1:1 *w/w* manually mixed) were weighed (5 to 10 mg) in aluminum pans. Samples were heated from 20 to 300 °C at 20 °C  $\text{min}^{-1}$  under a nitrogen flow of 50  $\text{mL}\cdot\text{min}^{-1}$ . FTIR spectra analysis (PerkinElmer, Norwalk, CT, USA) was performed from 4000 to 450  $\text{cm}^{-1}$ , using a KBr disk with 1% finely ground samples in order to identify chemical interactions between phlorotannin and PVP. X-ray powder diffraction patterns of phlorotannin, PVP, physical mixture of phlorotannin and PVP, PPNPS (1:6), PPNPS (1:8) and PPNPS (1:10) were taken at ambient temperature and were obtained with an X-ray diffractometer (XRD7000, JEOL, Tokyo, Japan). The amount of phlorotannin in all samples was the same. The following conditions were used: X-ray tube target of Cu, voltage of 40.0 (kV), current of 30.0 (mA), divergence slit of 1.0 (deg), scatter slit of 1.0 (deg), receiving slit of 0.3 (mm), drive axis of Theta-2, scan range of 10.0–70.0, scan mode of Continuous Scan, scan speed of 5.0 (deg/min), sampling pitch of 0.02 (deg) and preset time of 0.24 (sec). Morphological characterization of the nanoparticles was performed using TEM (JEM 2100, Shimadzu Corporation, Japan). Diluted samples were dripped onto 300 mesh parlodium-covered copper grids and were stained with 2% uranium acetate. Grids were dried at room temperature and then analyzed.

### 3.4. Determination of Stability

Phlorotannin and PPNPS with different ratios of 1:6, 1:8, 1:10 with added water were kept at room temperature  $22 \pm 3$  °C without light irradiation for 15 days to observe the storage stability.

### 3.5. Determination of Controlled Release In Vitro

In vitro release experiments of the encapsulated phlorotannin were carried out under two simulated digestive fluids. According to Oliyaei's methods [31] with minor modifications, 0.1 M HCl solution of pH 1.2 with pepsin (0.3% *w/v*) was used as a SGF and 0.1 M  $\text{NaHCO}_3$  solution of pH 7.5 with pancreatin (0.1% *w/v*) was used as a SIF. Approximately 0.5 g of PPNPS (1:8) was added to 10 mL SGF and vortexed in the dark for 120 min. The system was maintained at 37 °C under shaking, then immersed in 10 mL of SIF and incubated under the same condition for 240 min. A sample was taken every 30 min. The release of phlorotannin was determined using high-performance liquid chromatography (HPLC, Shimadzu SPD 20A, Japan). Methanol was used as the mobile phase at 0.8  $\text{mL}\cdot\text{min}^{-1}$ , in a  $\text{C}_{18}$  column (4.6 × 250 mm and particle size of 5  $\mu\text{m}$ ) at 40 °C. The elution gradient went from 100 to 85% methanol in 10 min. Detection was performed by a diode array detector (DAD) at 254 nm. The release of the phlorotannin was calculated according to Equation (1):

$$\text{Fractional release (\%)} = (1 - M_t/M_0) \times 100 \quad (1)$$

where  $M_0$  is the amount of phlorotannin initially encapsulated and  $M_t$  is the amount of phlorotannin remaining in the carriers at a given incubation time.

### 3.6. Cell Culture

HaCaT keratinocytes were thoroughly mixed in DMEM medium supplemented with 10% fetal bovine serum, 100 U/mL penicillin and 100 U/mL streptomycin, and cultured in a humidified atmosphere of 5% CO<sub>2</sub> at 37 °C according to the instructions from Shanghai Tongpai Technology Co., Ltd. When the cells reached a certain degree of confluence, they were washed with PBS for dead cells, digested with trypsin-EDTA, diluted to a suspension in fresh medium and set aside.

### 3.7. Antioxidant Activity Analysis

A total of 100 µL of HaCaT keratinocytes ( $1 \times 10^5$ /mL) was seeded onto a 96-well microtiter plate. After incubation in 5% CO<sub>2</sub> incubator at 37 °C for 24 h, the cells were treated with 1mM hydrogen peroxide (H<sub>2</sub>O<sub>2</sub>) for 1 h or without treatment (control). Then the cells were treated with varying concentrations of PPNPS (1:8) for another 23 h in 5% CO<sub>2</sub> incubator at 37 °C. Then cells were incubated with MTT (5 mg/mL) for 4 h to stain the cells. The MTT solution was then removed and 150 µL dimethyl sulfoxide (DMSO) was added and shaken well. The absorbance at 570 nm was determined by a microplate reader (Tecan Infinite, Männedorf, Switzerland). The control group refers to the cells without any treatment. The results were calculated and expressed as the cell viability according to Equation (2):

$$\text{Cell viability (\%)} = (A_{\text{sample}}/A_{\text{control}}) \times 100 \quad (2)$$

### 3.8. Intracellular ROS Detection

The generation of reactive oxygen species (ROS) was measured according to previous reports [34,35] with slight modifications. ROS can be evaluated by testing changes in fluorescence intensity of H<sub>2</sub>DCFDA, which is the most commonly applied method for quantitative examination of intracellular ROS. The intensity of green fluorescence is proportional to the level of ROS. HaCaT keratinocytes with a density of  $1.0 \times 10^5$  cells/mL were seeded in a 12-well plate (2 mL/well) for 24 h at 37 °C in a humidified incubator containing 5% CO<sub>2</sub>. Then, cells were treated with 1 mM H<sub>2</sub>O<sub>2</sub> for 1 h then the cells were dealt with varying concentrations of PPNPS (1:8) for another 1 h in 5% CO<sub>2</sub> incubator at 37 °C. The control group meant the cells without any treatment. Finally, treated cells were incubated with H<sub>2</sub>DCFDA for 30 min in PBS in 5% CO<sub>2</sub> incubator at 37 °C. The fluorescence intensity at varying circumstances was tracked by a fluorescent inverted microscope (Olympus IX73, Kyoto, Japan).

HaCaT keratinocytes with a density of  $1.0 \times 10^5$  cells/mL were seeded in a 12-well plate (2 mL/well) for 24 h at 37 °C in a humidified incubator containing 5% CO<sub>2</sub>. Then, cells were treated with 1 mM H<sub>2</sub>O<sub>2</sub> for 1 h then the cells were treated with varying concentrations of PPNPS (1:8) for another 1 h in 5% CO<sub>2</sub> incubator at 37 °C. The control group meant the cells without any treatment. Finally, treated cells were incubated with H<sub>2</sub>DCFDA for 30 min in PBS in 5% CO<sub>2</sub> incubator at 37 °C. After these treatments, cells were washed in PBS, trypsinized and collected by centrifugation. Then the cells were washed twice more before fixing with PBS, and were evenly distributed in a 96-well fluorescent plate. ROS production values were determined by a fluorescence microplate reader (Tecan Infinite 200 pro, Switzerland); the excitation wavelength was 485 nm and the emission wavelength was 535 nm. ROS production was calculated according to Equation (3):

$$\text{ROS production (\%)} = (A_{\text{sample group}}/A_{\text{H}_2\text{O}_2 \text{ group}}) \times 100 \quad (3)$$

### 3.9. In Vitro Cytotoxicity

The MTT assay was used to measure cell metabolic activity, cytotoxicity, proliferation and viability. Cell viability was determined by measuring the amount of tetrazolium salt in the viable cells of each sample using untreated cells as controls [36]. A cell culture model was used to determine the relative cytotoxicity of the nanoparticles by cell viability according to Liu et al.'s methods [37]. In a nutshell, 100  $\mu\text{L}$  of HaCaT keratinocytes ( $1 \times 10^5/\text{mL}$ ) was seeded onto a 96-well microtiter plate at 37 °C in a humidified atmosphere with 5%  $\text{CO}_2$  for 24 h. The cells were treated with varying concentrations of PPNPS for another 24 h. The control group meant the cells without any treatment. Then cells were incubated with MTT (5 mg/mL) for 4 h to stain the cells. The MTT solution was then removed and 150  $\mu\text{L}$  dimethyl sulfoxide (DMSO) was added and shaken well. The absorbance at 570 nm was determined by a microplate reader (Tecan Infinite, Switzerland). The results were calculated and expressed as the cell viability according to Equation (4):

$$\text{Cell viability (\%)} = (A_{\text{sample}}/A_{\text{control}}) \times 100 \quad (4)$$

### 3.10. Statistical Analysis

Each experiment was repeated at least 3 times and analyzed for variance. The results were expressed as the means  $\pm$  standard deviation. All data were performed with a one-way analysis of variance (ANOVA) and analyzed by SPSS 16.0 (SPSS Inc., 2001, Chicago, IL, USA) where  $p < 0.05$  was considered as the significance level.

## 4. Conclusions

In this study, phlorotannin was encapsulated in PVP shells to form PPNPS with relatively small, smooth spheres which were analyzed by TEM. The physicochemical characteristics which were analyzed by FTIR, DSC, X-ray and embedding rate proved that the best ratio of phlorotannin to PVP was 1:8 when phlorotannin was effectively encapsulated. DSC and X-ray analysis also showed that the phlorotannin was encapsulated inside the nanoparticles in an amorphous state, which should enhance its solubility and bioavailability. A sustained kinetic release profile was observed for the PPNPS in simulated GI conditions. Moreover, the PPNPS exhibited an outstanding antioxidant activity on HaCaT keratinocytes. In conclusion, our study demonstrated that PPNPS has the potential to be used as an effective oral delivery vehicle as well as in cosmetics to protect oxidative damage to the skin. The present work established a baseline for further investigation. In the next step, we will conduct an in vivo study to evaluate antioxidant activities of the nanoencapsulation.

**Author Contributions:** H.Q. conceived, designed and supervised the study. Y.B. performed the experiments and drafted the manuscript. Y.S. participated in the experiments. Y.G. performed experiments and data analysis. J.Z. and C.Y. participated the experimental design and reviewed the manuscript. All authors have read and agreed to the published version of the manuscript.

**Funding:** This research was funded by The National Key Research and Development Program of China (grant number 2019YFD0902001), Dalian Outstanding Young Science and Technology Talents Project (grant number 2018RL07) and Young Top Talents in the Xingliao Talents Program of Liaoning Province (grant number XLYC 1807166).

**Conflicts of Interest:** The authors declare no conflict of interest.

### Abbreviations

PPNPS	phlorotannin@pvp nanoparticles
ROS	reactive oxygen species
PVP	polyvinylpyrrolidone

TEM	transmission electron microscopy
FTIR	fourier transform infrared
DMEM	Dulbecco's Minimum Essential Medium
FBS	fetal bovine serum
DMSO	dimethyl sulfoxide
H <sub>2</sub> DCFDA	2',7'-dichlorodihydrofluorescein diacetate
DSC	differential scanning calorimetry
XRD	X-ray diffraction analysis
HPLC	high-performance liquid chromatography

## References

1. Balboa, E.M.; Conde, E.; Moure, A.; Falque, E.; Dominguez, H. In vitro antioxidant properties of crude extracts and compounds from brown algae. *Food Chem.* **2013**, *138*, 1764–1785. [[CrossRef](#)] [[PubMed](#)]
2. Lopes, G.; Barbosa, M.; Vallejo, F.; Gil-Izquierdo, Á.; Andrade, P.B.; Valentão, P.; Pereira, D.M.; Ferreres, F. Profiling phlorotannins from *Fucus* spp. of the Northern Portuguese coastline: Chemical approach by HPLC-DAD-ESI/MS and UPLC-ESI-QTOF/MS. *Algal Res.* **2018**, *29*, 113–120. [[CrossRef](#)]
3. Yang, Y.I.; Woo, J.H.; Seo, Y.J.; Lee, K.T.; Lim, Y.; Choi, J.H. Protective Effect of Brown Alga Phlorotannins against Hyper-inflammatory Responses in Lipopolysaccharide-Induced Sepsis Models. *J. Agric. Food Chem.* **2016**, *64*, 570–578. [[CrossRef](#)] [[PubMed](#)]
4. Nagayama, K.; Iwamura, Y.; Shibata, T.; Hirayama, I.; Nakamura, T. Bactericidal activity of phlorotannins from the brown alga *Ecklonia kurome*. *J. Antimicrob. Chemother.* **2002**, *50*, 889–893. [[CrossRef](#)] [[PubMed](#)]
5. Dong, X.; Bai, Y.; Xu, Z.; Shi, Y.; Sun, Y.; Janaswamy, S.; Yu, C.; Qi, H. Phlorotannins from *Undaria pinnatifida* Sporophyll: Extraction, Antioxidant, and Anti-Inflammatory Activities. *Mar. Drugs* **2019**, *17*, 434. [[CrossRef](#)]
6. Wang, T.; Jonsdottir, R.; Liu, H.; Gu, L.; Kristinsson, H.G.; Raghavan, S.; Olafsdottir, G. Antioxidant capacities of phlorotannins extracted from the brown algae *Fucus vesiculosus*. *J. Agric. Food Chem.* **2012**, *60*, 5874–5883. [[CrossRef](#)]
7. Kim, H.; Kong, C.S.; Lee, J.I.; Kim, H.; Baek, S.; Seo, Y. Evaluation of inhibitory effect of phlorotannins from *Ecklonia cava* on triglyceride accumulation in adipocyte. *J. Agric. Food Chem.* **2013**, *61*, 8541–8547. [[CrossRef](#)]
8. Artan, M.; Li, Y.; Karadeniz, F.; Lee, S.H.; Kim, M.M.; Kim, S.K. Anti-HIV-1 activity of phloroglucinol derivative, 6,6'-bieckol, from *Ecklonia cava*. *Bioorg. Med. Chem.* **2008**, *16*, 7921–7926. [[CrossRef](#)]
9. Ahn, J.H.; Yang, Y.I.; Lee, K.T.; Choi, J.H. Dieckol, isolated from the edible brown algae *Ecklonia cava*, induces apoptosis of ovarian cancer cells and inhibits tumor xenograft growth. *J. Cancer Res. Clin. Oncol.* **2015**, *141*, 255–268. [[CrossRef](#)]
10. Kong, C.S.; Kim, J.A.; Yoon, N.Y.; Kim, S.K. Induction of apoptosis by phloroglucinol derivative from *Ecklonia Cava* in MCF-7 human breast cancer cells. *Food Chem. Toxicol.* **2009**, *47*, 1653–1658. [[CrossRef](#)]
11. Yang, Y.I.; Ahn, J.H.; Choi, Y.S.; Choi, J.H. Brown algae phlorotannins enhance the tumoricidal effect of cisplatin and ameliorate cisplatin nephrotoxicity. *Gynecol. Oncol.* **2015**, *136*, 355–364. [[CrossRef](#)] [[PubMed](#)]
12. Ranganathan, A.; Hindupur, R.; Vallikannan, B. Biocompatible lutein-polymer-lipid nanocapsules: Acute and subacute toxicity and bioavailability in mice. *Mater. Sci. Eng. C Mater. Biol. Appl.* **2016**, *69*, 1318–1327. [[CrossRef](#)] [[PubMed](#)]
13. Donsì, F.; Sessa, M.; Mediouni, H.; Mgaidi, A.; Ferrari, G. Encapsulation of bioactive compounds in nanoemulsion- based delivery systems. *Procedia Food Sci.* **2011**, *1*, 1666–1671. [[CrossRef](#)]
14. Donsi, F.; Wang, Y.; Li, J.; Huang, Q. Preparation of curcumin sub-micrometer dispersions by high-pressure homogenization. *J. Agric. Food Chem.* **2010**, *58*, 2848–2853. [[CrossRef](#)] [[PubMed](#)]
15. Je, H.J.; Kim, E.S.; Lee, J.S.; Lee, H.G. Release Properties and Cellular Uptake in Caco-2 Cells of Size-Controlled Chitosan Nanoparticles. *J. Agric. Food Chem.* **2017**, *65*, 10899–10906. [[CrossRef](#)]
16. Dos Santos, P.D.F.; Francisco, C.R.L.; Coqueiro, A.; Leimann, F.V.; Pinela, J.; Calhelha, R.C.; Porto Ineu, R.; Ferreira, I.; Bona, E.; Goncalves, O.H. The nanoencapsulation of curcuminoids extracted from *Curcuma longa* L. and an evaluation of their cytotoxic, enzymatic, antioxidant and anti-inflammatory activities. *Food Funct.* **2019**, *10*, 573–582. [[CrossRef](#)]

17. Gupta, B.S.; Chen, B.-R.; Lee, M.-J. Solvation consequences of polymer PVP with biological buffers MES, MOPS, and MOPSO in aqueous solutions. *J. Chem. Thermodyn.* **2015**, *91*, 62–72. [CrossRef]
18. Kowalonek, J.; Kaczmarek, H. Studies of pectin/polyvinylpyrrolidone blends exposed to ultraviolet radiation. *Eur. Polym. J.* **2010**, *46*, 345–353. [CrossRef]
19. Chen, Y.; Xue, J.; Luo, Y. Encapsulation of Phloretin in a Ternary Nanocomplex Prepared with Phytoglycogen-Caseinate-Pectin via Electrostatic Interactions and Chemical Cross-Linking. *J. Agric. Food Chem.* **2020**. [CrossRef]
20. Cai, L.; Cao, M.; Regenstein, J. Slow-Release and Nontoxic Pickering Emulsion Platform for Antimicrobial Peptide. *J. Agric. Food Chem.* **2020**, *68*, 7453–7466. [CrossRef]
21. Zhu, J.; Li, H.; Xu, Y.; Wang, D. Construction of Fucoxanthin Vector Based on Binding of Whey Protein Isolate and Its Subsequent Complex Coacervation with Lysozyme. *J. Agric. Food Chem.* **2019**, *67*, 2980–2990. [CrossRef] [PubMed]
22. Ragan, M.; Glombitza, K. Phlorotannins, brown algal polyphenols. *Prog. Phycol. Res.* **1986**, 129–241. Available online: <http://espace.library.uq.edu.au/view/UQ:321862> (accessed on 28 September 2020).
23. do Prado Silva, J.T.; Geiss, J.M.T.; Oliveira, S.M.; Brum, E.D.S.; Sagae, S.C.; Becker, D.; Leimann, F.V.; Ineu, R.P.; Guerra, G.P.; Goncalves, O.H. Nanoencapsulation of lutein and its effect on mice's declarative memory. *Mater. Sci. Eng. C Mater. Biol. Appl.* **2017**, *76*, 1005–1011. [CrossRef] [PubMed]
24. Wang, L.; Li, X.; Wang, H. Fabrication of BSA-Pinus koraiensis polyphenol-chitosan nanoparticles and their release characteristics under in vitro simulated gastrointestinal digestion. *Food Funct.* **2019**, *10*, 1295–1301. [CrossRef] [PubMed]
25. Slika, L.; Moubarak, A.; Borjac, J.; Baydoun, E.; Patra, D. Preparation of curcumin-poly (allyl amine) hydrochloride based nanocapsules: Piperine in nanocapsules accelerates encapsulation and release of curcumin and effectiveness against colon cancer cells. *Mater. Sci. Eng. C Mater. Biol. Appl.* **2020**, *109*, 110550. [CrossRef]
26. Liu, Z.; Hu, Y.; Li, X.; Mei, Z.; Wu, S.; He, Y.; Jiang, X.; Sun, J.; Xiao, J.; Deng, L.; et al. Nanoencapsulation of Cyanidin-3-O-glucoside Enhances Protection Against UVB-Induced Epidermal Damage through Regulation of p53-Mediated Apoptosis in Mice. *J. Agric. Food Chem.* **2018**, *66*, 5359–5367. [CrossRef]
27. Liu, C.; Zhang, S.; McClements, D.J.; Wang, D.; Xu, Y. Design of Astaxanthin-Loaded Core-Shell Nanoparticles Consisting of Chitosan Oligosaccharides and Poly(lactic-co-glycolic acid): Enhancement of Water Solubility, Stability, and Bioavailability. *J. Agric. Food Chem.* **2019**, *67*, 5113–5121. [CrossRef]
28. Wang, X.; Zhou, Z.; Guo, X.; He, Q.; Hao, C.; Ge, C. Ultrasonic-assisted synthesis of sodium lignosulfonate-grafted poly(acrylic acid-co-poly(vinyl pyrrolidone)) hydrogel for drug delivery. *RSC Adv.* **2016**, *6*, 35550–35558. [CrossRef]
29. Huang, S.; He, J.; Cao, L.; Lin, H.; Zhang, W.; Zhong, Q. Improved Physicochemical Properties of Curcumin-Loaded Solid Lipid Nanoparticles Stabilized by Sodium Caseinate-Lactose Maillard Conjugate. *J. Agric. Food Chem.* **2020**, *68*, 7072–7081. [CrossRef]
30. Lee, M.H.; Park, H.J. Preparation of halloysite nanotubes coated with Eudragit for a controlled release of thyme essential oil. *J. Appl. Polym. Sci.* **2015**, *132*. [CrossRef]
31. Oliyaei, N.; Moosavi-Nasab, M.; Tamaddon, A.M.; Fazaeli, M. Encapsulation of fucoxanthin in binary matrices of porous starch and halloysite. *Food Hydrocoll.* **2020**, *100*, 105458. [CrossRef]
32. Reuter, S.; Gupta, S.C.; Chaturvedi, M.M.; Aggarwal, B.B. Oxidative stress, inflammation, and cancer: How are they linked? *Free Radic. Biol. Med.* **2010**, *49*, 1603–1616. [CrossRef] [PubMed]
33. Djilas, S.; Canadanovic-Brunet, J.; Cetkovic, G. By-products of fruits processing as a source of phytochemicals. *Chem. Ind. Chem. Eng. Q.* **2009**, *15*, 191–202. [CrossRef]
34. Hu, Q.; Yuan, B.; Xiao, H.; Zhao, L.; Wu, X.; Rakariyatham, K.; Zhong, L.; Han, Y.; Muinde Kimatu, B.; Yang, W. Polyphenols-rich extract from *Pleurotus eryngii* with growth inhibitory of HCT116 colon cancer cells and anti-inflammatory function in RAW264.7 cells. *Food Funct.* **2018**, *9*, 1601–1611. [CrossRef]
35. Yuan, B.; Zhao, L.; Rakariyatham, K.; Han, Y.; Gao, Z.; Muinde Kimatu, B.; Hu, Q.; Xiao, H. Isolation of a novel bioactive protein from an edible mushroom *Pleurotus eryngii* and its anti-inflammatory potential. *Food Funct.* **2017**, *8*, 2175–2183. [CrossRef]

36. Liu, C.; Zhang, Z.; Kong, Q.; Zhang, R.; Yang, X. Enhancing the antitumor activity of tea polyphenols encapsulated in biodegradable nanogels by macromolecular self-assembly. *RSC Adv.* **2019**, *9*, 10004–10016. [[CrossRef](#)]
37. Liu, S.; You, L.; Zhao, Y.; Chang, X. Hawthorn Polyphenol Extract Inhibits UVB-Induced Skin Photoaging by Regulating MMP Expression and Type I Procollagen Production in Mice. *J. Agric. Food Chem.* **2018**, *66*, 8537–8546. [[CrossRef](#)]



© 2020 by the authors. Licensee MDPI, Basel, Switzerland. This article is an open access article distributed under the terms and conditions of the Creative Commons Attribution (CC BY) license (<http://creativecommons.org/licenses/by/4.0/>).